CR 82.010

NAVAL CIVIL ENGINEERING LABORATORY
Port Hueneme, California

Sponsored by
CHIEF OF NAVAL MATERIAL

A REVIEW OF ADDED MASS AND FLUID INERTIAL FORCES

January 1982

An Investigation Conducted by
C. E. Brennen
360 Olive Tree Lane
Sierra Madre, California

N62583-81-MR-554

Approved for public release; distribution unlimited

Unclassified
SECURITY CLASSIFICATION OF THIS PAGE (When Data Entered)

REPORT DOCUMENTATION PAGE		READ INSTRUCTIONS BEFORE COMPLETING FORM
1. REPORT NUMBER CR 82.010	2. GOVT ACCESSION NO.	3. RECIPIENT'S CATALOG NUMBER
4. TITLE (and Subtitle) A Review of Added Mass and Fluid Inertial Forces		5. TYPE OF REPORT & PERIOD COVERED Final Apr 1981 - Nov 1981
		6. PERFORMING ORG. REPORT NUMBER
7. AUTHOR(s) C. E. Brennen		8. CONTRACT OR GRANT NUMBER(s) N62583-81-MR-554
9. PERFORMING ORGANIZATION NAME AND ADDRESS C. E. Brennen 360 Olive Tree Lane Sierra Madre, CA 91024		10. PROGRAM ELEMENT, PROJECT, TASK AREA & WORK UNIT NUMBERS PE61152N ZR000-01-184
11. CONTROLLING OFFICE NAME AND ADDRESS Naval Civil Engineering Laboratory Port Hueneme, CA 93043		12. REPORT DATE January 1982
		13. NUMBER OF PAGES 50
14. MONITORING AGENCY NAME & ADDRESS(if different from Controlling Office)		15. SECURITY CLASS. (of this report) Unclassified
		15a. DECLASSIFICATION DOWNGRADING SCHEDULE

16. DISTRIBUTION STATEMENT (of this Report)

Approved for public release; distribution unlimited

17. DISTRIBUTION STATEMENT (of the abstract entered in Block 20, if different from Report)

18. SUPPLEMENTARY NOTES

19. KEY WORDS (Continue on reverse side if necessary and identify by block number)

Fluid mechanics, Fluid-structure interaction, Added mass, Fluid inertial forces, Ocean engineering

20. ABSTRACT (Continue on reverse side if necessary and identify by block number)

This report reviews the existing state of knowledge concerning the evaluation of the forces imposed on a body in a fluid due to acceleration of either the body or the fluid. It concentrates on those fluid inertial forces due to acceleration rather than on the drag/lift forces due to steady motion. The first part of the report presents a survey of the analytical

DD FORM 1 JAN 73 1473 EDITION OF 1 NOV 65 IS OBSOLETE

Unclassified
SECURITY CLASSIFICATION OF THIS PAGE (When Data Entered)

background including the definition of added mass, the structure of the added mass matrix and other effects such as the influence of viscosity, fluid compressibility and the proximity of solid and free surface boundaries. Then the existing data base from experiments and potential flow calculations is reviewed. Approximate empirical methods for bodies of complex geometry are explored in a preliminary way. The possible dramatic effects of the proximity of the ocean bottom are further highlighted. The confused state of affairs regarding the possibly major effects of viscosity in certain regimes of frequency and Reynolds number is discussed. Finally a number of recommendations stemming from ocean engineering problems are put forward.

CC BY

CONTENTS

CC BY

cc BY

1. INTRODUCTION

Whenever acceleration is imposed on a fluid flow either by acceleration of a body or by acceleration externally imposed on the fluid, additional fluid forces will act on the surfaces in contact with the fluid. These fluid inertial forces can be of considerable importance in many ocean engineering problems. The purpose of this report is to review some of the characteristics of these fluid inertial forces and, in particular, to evaluate the state of knowledge of the "added mass" matrices which are used to characterize the forces. The first part of the report (Section 3) is also intended to serve educational purposes. The second part (Section 4) reviews the existing data base and some of the areas in which there is either a lack of data or a data base which is contradictory. It is also intended to convey the limitations of the existing knowledge. Finally a number of suggestions for improvement in our present understanding are listed in the concluding section.

Unlike many reviews, the author has not attempted to absorb every publication on the subject. Rather the time which would have been spent on such an effort, was devoted to more concentrated analysis of the subject. Other excellent reviews of various aspects of unsteady fluid forces exist; in particular the reader is referred to the recent books by Blevins (Ref.18) and by Sarpkaya and Isaacson (Ref.17).

2. GENERAL EXPLANATION OF ADDED MASS

Perhaps the simplest view of the phenomenon of "added mass" is that it determines the necessary work done to change the kinetic energy associated with the motion of the fluid. Any motion of a fluid such as that which occurs when a body moves through it implies a certain positive, non-zero amount of kinetic energy associated with the fluid motions. This kinetic energy, T, can be simply represented by

$$T=\frac{\rho}{2}\int_V(u_1^2+u_2^2+u_3^2)dV=\frac{\rho}{2}\int_V u_i u_i dV \tag{1}$$

where the $u_i (i=1,2,3)$ represent the Cartesian components of fluid velocity and V is the entire domain or volume of fluid. For simplicity we shall assume throughout that the fluid is incompressible with a density ρ.

If the motion of the body is one of steady rectilinear translation at velocity, U, through a fluid otherwise at rest then clearly the amount of kinetic energy, T, remains constant with time. Furthermore it is clear that T will in some manner be proportional to the square of the velocity, U, of translation. Indeed if the flow is such that when U is altered the velocity, u_i, at each point in fluid relative to the body varies in direct proportion to U then T could conveniently be expressed as

$$T=\rho\frac{I}{2}U^2 \quad \text{where} \quad I=\int_V\frac{u_i}{U}\frac{u_i}{U}dV \tag{2}$$

and the integral I would be a simple invariant number. This is indeed the case with some fluid flow solutions such as potential flow and low Reynolds number Stokes flow. However it may not be true for the complex, vortex shedding flows which occur at intermediate Reynolds numbers.

Now consider that the body begins to accelerate or decelerate. Clearly the kinetic energy in the fluid will also begin to change as U changes. If the body is accelerated then the kinetic energy will in all probability increase. But this energy must be supplied; additional work must be done on the fluid by the body in order to increase the kinetic energy of the fluid. And the rate of additional work required is simply the rate of change of T with respect to time, dT/dt. This additional work is therefore experienced by the body as an additional drag, F, such that the rate of additional work done, $-FU$ is simply

CC BY

equal to dT/dt. If the pattern of flow is not changing such that the integral I remains constant it follows that the "added drag", F, is simply

$$F = -\frac{1}{U}\frac{dT}{dt} = -\rho\, I\, \frac{dU}{dt} \tag{3}$$

Now this force has the same form and sign as that required to accelerate the mass (m) of the body itself, namely $m\frac{dU}{dt}$. Consequently it is often convenient to visualize the mass of fluid ρI, as an "added mass", M, of fluid which is being accelerated with the body. Of course, there is no such identifiable fluid mass; rather all of the fluid is accelerating to some degree such that the total kinetic energy of the fluid is increasing.

It is important to stress that F is not the only drag force experienced by the body. During steady translation in a real viscous fluid there is a steady drag associated with the necessary work which must be done to balance the steady rate of dissipation of energy in the viscous fluid. When the body accelerates there will be a similar though not necessarily equal drag associated with the instantaneous value of U. Furthermore there may be delayed effects associated with the entire previous history of translation (e.g. the Basset force, Ref.1, p.375).

CC BY

3. ANALYTICAL APPROACHES TO ADDED MASS

3.1 EXAMPLES: RECTILINEAR MOTION OF A SPHERE AND CYLINDER WITH POTENTIAL FLOW

In the preceding discussion the consequences of acceleration were illustrated by reference to simple rectilinear motion of velocity, U. It should be clear that the methodology could be extended to more general motions and indeed this will be carried out in the following section. But prior to this it is worth illustrating how the integral, I, and therefore the added mass can be calculated for rectilinear motion. For the purposes of this example let us examine the idealized potential flows past a sphere and a cylinder. The geometry for both is as depicted in Fig.1. The sphere or cylinder of radius R is assumed to be moving with time varying velocity $U(t)$ (t is time) in the positive x direction. Polar coordinates (r, ϑ) are used where $x = r\cos\vartheta$

Fig.1

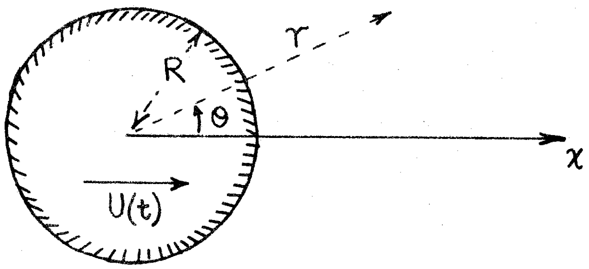

The resulting fluid velocities u_r, u_ϑ in the r and ϑ directions are then given by a velocity potential, φ, such that

$$u_r = \frac{\partial \varphi}{\partial r} \; ; \; u_\vartheta = \frac{1}{r}\frac{\partial \varphi}{\partial \vartheta} \tag{4}$$

and the appropriate velocity potentials in the two cases are

$$\varphi_{sphere} = -\frac{UR^3}{2r^2}\cos\vartheta \tag{5}$$

$$\varphi_{cylinder} = -\frac{UR^2}{r}\cos\vartheta$$

The reader who is unfamiliar with these solutions may wish to satisfy himself that two solutions satisfy (i) Laplaces equation, $\nabla^2\varphi = 0$, in spherical and cylindrical coordinates respectively and (ii) the boundary condition that the relative velocity normal to the surface of the body is zero ($(u_r)_{r=R} = U\cos\vartheta$).

CC BY

It follows that these flows are of the type in which u_i is directly proportional to U and consequently the integrals, I, can be evaluated as

$$\textit{Sphere}: I=\int_R^\infty\int_0^\pi\left[\left(\frac{1}{U}\frac{\partial\varphi}{\partial r}\right)^2+\left(\frac{1}{Ur}\frac{\partial\varphi}{\partial\vartheta}\right)^2\right]2\pi r^2\sin\vartheta\, d\vartheta dr=\frac{2}{3}\pi R^3 \tag{7}$$

$$\textit{therefore}\quad M=\frac{2}{3}\pi R^3\rho$$

$$\textit{Cylinder}:\ I=\int_R^\infty\int_0^{2\pi}\left[\left(\frac{1}{U}\frac{\partial\varphi}{\partial r}\right)^2+\left(\frac{1}{Ur}\frac{\partial\varphi}{\partial\vartheta}\right)^2\right]r d\vartheta dr=\pi R^2\quad \textit{per unit length} \tag{8}$$

$$\textit{therefore}\quad M=\pi R^2\rho\quad \textit{per unit length.}$$

Note that the added mass, M, of the cylinder is equal to the mass of the fluid displaced by the body, whereas the added mass of the sphere is one half of the displaced mass.

These are algebraically the simplest potential flows for which the value of I can be evaluated. However, it is conceptually simple to visualize how I could be evaluated for any flow provided the flow solution (the u_i/U values) are available. Note that, in effect, one need only have available the solution for the steady flow in the direction under consideration. This considerably simplifies the added mass calculation for rectilinear motion. Later we shall examine the more general case of arbitrary motion.

3.2 RELATION TO DISPLACED MASS; VARIATION WITH DIRECTION OF ACCELERATION

In the preceding section it was noted that in the ideal case of potential flow around a circular cylinder in rectilinear motion the added mass is equal to the mass of fluid displaced by the cylinder. This should be regarded as coincidental. There is no general correlation between added mass and displaced fluid mass. As we have seen the added mass for a sphere is one half of the displaced fluid mass. Furthermore the idealized potential flow past an infinitely thin flat plate (zero displaced fluid mass) accelerated normal to itself has an added mass equal to the mass of a circular cylinder of fluid with a diameter equal to the width of the plate.

Thus the displaced fluid mass may not even be a good first approximation to the added mass (except for the case of the circular cylinder). Furthermore we shall see that, in general, the value of the added mass depends on the direction of acceleration. For example, the idealized potential flow solution for the infinitely thin flat plate accelerated in a tangential rather than a normal direction yields zero added mass rather than the value described above. A review of the available data suggests that a better (but still very crude) first approximation to the added mass of a body for a given direction of acceleration would be the mass of the fluid volume obtained by taking the projected area of the body in that direction and evaluating one half of the volume of the sphere with the same projected area (see Sections 4.2, 4.3). An improvement on this is included in Section 4.2.

One other complication will emerge in the following section when the complete added mass matrix is defined, namely that the force on the body due to acceleration is not necessarily in the same direction as the acceleration. For an unsymmetric body acceleration in one direction can give rise to an "added mass" effect resulting in a force which has a component in a direction perpendicular to the direction of acceleration. If, for example, one were lifting a body from the ocean bottom by means of a cable then an increase in the lift rate could produce a lateral motion of the body.

3.3 THE ADDED MASS MATRIX

Up to this point, most of the examples and discussion have centered on simple rectilinear motion. However in general the response of a body to an additional force applied at some point and in some direction will not be confined to motion in that same direction. Instead there will be a general induced acceleration of the body consisting of three translation accelerations, A_j, $j=1,2,3$ in three perpendicular directions and three angular accelerations, A_j, $j=4,5,6$. Then the added mass matrix M_{ij}, $i=1\rightarrow 6$, $j=1\rightarrow 6$ provides a method of expressing the relationship between the six force components, F_i, imposed on the body by the inertial effects of the fluid due to the six possible components of acceleration,:

$$F_i=-M_{ij}A_j \tag{9}$$

The matrix M_{ij} must have added to it the inertial matrix due to the mass of the body in order to complete the formulation of the inertial forces. If the center of mass of the body is chosen as the origin the

CC BY

body mass matrix is symmetric and contains only seven different, non-zero values, namely the mass and the six different components of the moment-of-inertia matrix [Yih, p.102]. However one cannot in general relate any of the 36 different components of the added mass matrix nor prove that any of them are zero except in specific cases or for specific kinds of flow. Consequently an externally applied additional force will in general create acceleration in all six components of velocity and angular velocity. Thankfully it is rarely necessary to have to handle 36 different added mass coefficients. For potential flow one can show [Yih, p.100] that the added mass matrix must be symmetric; since the system is then conservative the symmetry also follows from the theorem of reciprocity. This reduces the number of coefficients to 21. However no further reduction is possible except for bodies with geometric symmetries.

The simplifications introduced by geometric symmetries of the body are fairly easily established. Consider for example a body with a single plane of symmetry, for example an airplane. It is clearly convenient to select axes such that this plane of symmetry corresponds say, the x_3=0 plane. Then any acceleration confined to this plane, namely any combination of A_1, A_2 and A_6 will produce no added mass force F_3, F_4 or F_5; the only possible non-zero forces will be F_1, F_2 and F_6. It follows that for such a body the following 9 components of the added mass matrix will be zero:

$$M_{ij}=0 \quad \text{for} \quad i=3,4,5\,;\ j=1,2,6 \tag{10}$$

If in addition the flow is assumed to be potential such that the matrix is symmetric then M_{ji}=0 for the same domains of i and J. The number of non-zero values required to define the matrix is 12, namely

$$M_{ii},\ i=1\rightarrow 6 \quad \text{and} \quad M_{12}, M_{34}, M_{35}, M_{45}, M_{16} \quad \text{and} \quad M_{26} \tag{11}$$

Bodies which have two planes of symmetry (for example a hemisphere) yield a further reduction in the number of non-zero values. Suppose axes are chosen such that both x_2=0 and x_3=0 are planes of symmetry. Then not only must (10) be true but also

$$M_{ij}=0 \quad \text{for} \quad i=2,4,6\,;\ j=1,3,5 \tag{12}$$

and again, assuming potential flow M_{ji}=0 for the same domains. Then the only non-zero values which

CC BY

need evaluation are

$$M_{ii}\ ,\ i=1\rightarrow 6 \text{ and } M_{26}\ ,M_{35} \tag{13}$$

The last two, which with $M_{62}=M_{26}$ and $M_{53}=M_{35}$ represent the only non-zero off-diagonal terms, correspond to the moment about the x_3 axis generated by acceleration in the x_2 direction and the moment about the x_2 axis generated by acceleration in the x_3 direction. In other words since the body is not symmetric about the x_2x_3 plane linear acceleration in either the x_2 or x_3 direction will cause pitching moments in the x_1x_2 or x_1x_3 planes.

A few simple bodies such as a sphere, circular cylinder, cube, rectangular box, etc have three planes of symmetry. By following the same procedure used above it is clear that the only possible non-zero elements are

$$M_{ii}\ ,\ i=1\rightarrow 6,\ M_{15},M_{16},M_{24},M_{26},M_{34},M_{35} \tag{14}$$

and that if potential flow is assumed all of the off-diagonal terms are zero. Only in this simple case of three axes of symmetry and symmetry of the matrix (see below for conditions on this) does the matrix become purely diagonal so that there are no secondary induced accelerations.

It remains to discuss the precise flow conditions under which the matrix can be assumed to be symmetric and then finally to indicate how all of the elements could be evaluated.

3.4 ADDED MASS MATRIX SYMMETRY AND SUPERPOSIBILITY OF FLOW SOLUTIONS

The astute reader will have recognized that the mere definition of M_{ij} in Eq.(9) requires certain assumptions concerning the nature of the flow and the ability to linearly superpose the effects (i.e. forces) of acceleration in the six directions. The question of the minimum preconditions necessary in order to write Equation (9) is one which will not be addressed here. It is however clear that these preconditions are met as soon as one makes the assumptions necessary to evaluate M_{ij}. To the authors knowledge the only evaluations which exist require that the fluid flow is superposable in the following sense; that the total induced fluid velocity can be obtained by linear addition of the fluid velocities caused by each of the components of the body motion or velocity. For this to be true requires that both the equations used to solve for the fluid flow and the boundary conditions be linear. This is not true in general of the Navier-Stokes equations for fluid motion and therefore superposability is not, in general, applicable. However there are two models of fluid flow which do satisfy this condition namely (i) the potential flow model for high Reynolds flow [Yih, p.100] and (ii) the Stokes flow model for asymptotically small Reynolds numbers. In both cases the equations of motion can be put in linear form. Furthermore provided if one is dealing with rigid or undeformable boundaries the boundary conditions are also linear. Only in these two limiting cases can the added mass matrix be regarded as an exact representation of the relation between fluid inertial force and body acceleration. In other types of flow it could however be regarded as a reasonable first approximation. Case (ii) above is of interest in flows such as occur in slurries or suspensions; however we shall from here on confine our remarks to case (i) which is of greater practical importance in ocean engineering.

When the flow is linearly superposable, it is convenient to define U_{ij} as the induced fluid velocity caused by unit velocity of the body in the j direction $(j=1\rightarrow 6)$. Included here are both the translation components, $j=1,2,3$, and rotational components, $j=4,5,6$ of body motion. Then if the body velocities are denoted by U_j, $j=1\rightarrow 6$, it follows that the fluid velocity

$$u_i=u_{ij}U_j \tag{15}$$

Consequently one can write Equation (1) as

$$T=\frac{1}{2}A_{jk}\ U_jU_k \tag{16}$$

where the matrix A_{jk} is composed of elements

$$A_{jk}=\rho\int u_{ij}u_{ik}dV=M_{jk} \tag{17}$$

It can be shown [Yih, p.102] that the matrix A_{jk} is in fact the added mass matrix M_{jk}. It is certainly clear that the diagonal terms A_{11}, A_{22}, A_{33} are identical to the added masses evaluated in Section 3. (To establish this define the direction x of Section 3 as either x_1, x_2 or x_3; then u_{ij} and u_{ik} are identical and equal to the velocity $\frac{u_i}{U}$ used in Section 3.)

CC BY

Furthermore it is clear from this evaluation that the added mass matrix must be symmetric since reversing j and k in Equation (16) does not change the value of the integral. Hence superposability implies symmetry of the added mass matrix.

3.5 EVALUATION OF THE ADDED MASS MATRIX

The expression (17) will permit the evaluation of the entire added mass matrix. Indeed it should be particularly noted that use of this result only requires the solution of steady flow problems since u_{ij} is the fluid velocity due to unit velocity of motion of the body in the j direction. Consequently the solution of six steady flows for $j=1\rightarrow 6$ allows evaluation of all 21 distinct values in the added mass matrix. Hence one can make use of existing methods for solving steady flows around bodies of quite complex geometry in order to evaluate the added mass matrix. References 1,2,3,4 and 9 provide information on these existing methods.

One other form of Equation (17) can also be valuable in dealing with potential flows. Then if φ_j represents the velocity potential of the steady flow due to unit motion of the body in the j-direction then it follows that

$$u_{ij}=\frac{\partial\varphi_j}{\partial x_i} \tag{18}$$

Substitution into Equation (17) and application of Green's theorem leads to

$$A_{jk}=-\rho\int_S \varphi_j \frac{\partial\varphi_k}{\partial n}\, dS \tag{19}$$

where n is the outward normal to the surface, S, which represents the body surface. In many cases of steady potential flows around complex bodies it is clearly easier to evaluate the surface integral in (19) than the volume integral in (17). Indeed the form (19) is ideally suited for use with potential flow codes such as the Douglas-Neuman code.

3.6 VELOCITY AND ACCELERATION OF THE FLUID RATHER THAN THE BODY

All of the preceding discussion was centered on the inertial forces due to acceleration of a body in a fluid. This review would be incomplete without some comment on the cases in which the fluid far

CC BY

from the body is either (i) moving with a constant, uniform velocity or (ii) accelerating.

Examine case (i) first. It was implicitly assumed in all the preceding sections that the fluid far from the body was at rest. Otherwise clearly the integral defining T (Eq.(1)) would have an infinite value and the subsequent analysis would be meaningless. If, as in case (i), the fluid far from the body has some uniform constant velocity denoted by W_i then it is clear that since the inertial force cannot be altered by a simple Galilean transformation it follows that the proper definition of T under these circumstances is

$$T=\frac{\rho}{2}\int_V (u_i - W_i)(u_i - W_i)\, dV \tag{20}$$

The value of this integral is then finite and the conundrum resolved. In other words the appropriate u_i to be used in Eq.(1) is the velocity of the fluid *relative to the fluid velocity far from the body,* provided the latter is constant with time. This leads to no alteration in fluid inertial forces. A rigorous expression for the forces would be

$$F_i=-M_{ij}\frac{d}{dt}(U_j - W_j)=-M_{ij}\frac{dU_j}{dt} \tag{21}$$

but since the time derivative of W_j is zero the original relation (9) is recovered.

However case (ii) in which W_j is a function of time is more complex. It is important to identify the fluid inertial forces in this case for two reasons. First it is of practical importance in analyzing, for example, ocean wave forces on structures. Secondly, many of the important experiments on unsteady forces are performed using an accelerating fluid rather than an accelerating body (e.g. Refs.10 and 11). We begin by visualizing a case (i) flow with a constant, uniform fluid velocity, W_j ($j=1\rightarrow 3$), far from a body whose center of volume is moving at a velocity, U_j ($j=1\rightarrow 6$). The body is also accelerating with components, A_j. The flow satisfies the Navier-Stokes equations for fluid motion and the solid body boundary conditions. The fluid inertial forces in this case are given by Eq.(21). Now consider a slightly different flow whose velocities are identical to those of the first flow but in which an additional uniform acceleration $j=1,2,3$ is applied globally to both the fluid and body. Now the actual acceleration of the body is $(A_j + \frac{dW_j}{dt})$. The Navier-Stokes equations of fluid motion and

CC BY

the solid body boundary conditions are identical for the two flows *except* that where the pressure, p, appears in the equations for the first flow, the expression $p-\rho x_j \frac{dW_j}{dt}$ appears in the equations for the second flow. Consequently the stresses and forces which the fluid exerts on the body are identical except for an additional contribution in the second flow due to the additional pressure, $\rho x_j \frac{dW_j}{dt}$. When this is integrated over the surface of the body the additional force on the body turns out to be $\rho V_D \frac{dW_j}{dt}$ where V_D is the volume of fluid displaced by the body. Consequently the inertial force is

$$F_i = -M_{ij}A_j + \rho V_D \frac{dW_i}{dt} \tag{22}$$

But as stated previously the acceleration of the body in the second flow is now $A_j + dW_j/dt$ and hence in the case of the second flow

$$\frac{dU_j}{dt} = A_j + \frac{dW_j}{dt} \tag{23}$$

where dW_j/dt is the acceleration of the fluid fa. from the body. Substitution for A_j in Eq.(22) produces the final required result for the second flow:

$$F_i = -M_{ij} \frac{dU_j}{dt} + (M_{ij} + \rho V_D \delta_{ij}) \frac{dW_j}{dt}, \quad j=1,2,3 \tag{24}$$

where δ_{ij} is the Kronecker delta ($\delta_{ij}=1$ for $i=j$, $\delta_{ij}=0$ for $i \neq j$).

Therefore the "added mass" associated with the *fluid* acceleration, dW_j/dt, in the second flow is the sum of the true added mass, M_{ij}, and a diagonal matrix with components equal to the mass of the displaced fluid, ρV_D.

However we must now examine more closely the general validity of Eq.(24). The first and second flows described above were *assumed* to have identical fluid velocity fields at the moment at which the forces were considered. This will *not* be true in general for solutions of the Navier-Stokes equation even though the body velocities and far field fluid velocities are identical. In general the solutions to the Navier-Stokes equations will also depend on all of the previous time history of the body and far

CC BY

field fluid motions and consequently the two flows will *not* in general have identical fluid velocity fields. There are however two important exceptions to this and in both cases Eq.(24) will be true. First if the viscous effects are neglected then the fluid has no memory and the fluid velocity fields will be identical; thus Eq.(24) holds for potential flows. Secondly if the previous history of the *relative* velocity, $(U_j - W_j)$ is identical in the two flows then (24) will hold regardless of viscous effects.

Therefore, in summary, the fluid inertial forces due to any combination of body or far field fluid acceleration $(dU_j/dt$ *or* $dW_j/dt)$ can be exactly represented by Eq.(24) if either (i) viscous effects are neglected or (ii) the matrix M_{ij} represents the fluid inertial forces for the case in which the fluid is at rest far from the body and the entire previous history of the relative motion $(U_j - W_j)$ is identical to that of the flow under consideration. The latter is indeed the case when comparing two cases, for example, in the first of which the far field fluid motion is sinusoidal in time and the body at rest and in the second of which the far field fluid motion is at rest and the body moves sinusoidally. Consequently the "added mass" in the experiments of Keulegan and Carpenter (Ref.10) in which the far field fluid is accelerated sinusoidally should yield $(M_{ii} + \rho V_D)$ whereas the experiments of Skop, Ramberg and Ferer (Ref.15) in which the body is accelerated should yield, M_{ii}. To transfer results from one case to the other requires the addition or subtraction of the displaced mass. For the examples of Section 3.1 the values of $(M_{ii} + \rho V_D)$ would be $2\rho\pi R^2$ per unit length in the case of the cylinder and $2\rho\pi R^3$ in the case of the sphere. Sometimes the total $(M_{ii} + \rho V_D)$ is referred to as the added mass and this can result in some confusion. Strictly speaking the term added mass should be reserved for M_{ij} only, or in other words the case in which the body is accelerating and not the far field fluid.

3.7 THE EFFECT OF A NEARLY SOLID BOUNDARY

The effects on the added mass due to the proximity of a solid boundary will be addressed in more detail later (see Section 4.4). It is generally true that the presence of the boundary tends to increase the added mass (see Tables I → V) and sometimes this increase can be very large. Here we merely remark that the preceding theoretical results are equally applicable in the presence of a solid boundary with the following addenda:

CC BY

A. The reductions due to geometric symmetries discussed in Section 3.3 only apply to total geometric symmetries of both the body and solid boundary.

B. Potential flows with a plane solid boundary can be modelled by reflecting the flow and body in the plane and treating the total flow due to the body and its image. Equivalence of the two problems allows the transference of added mass coefficients from one to the other. As an example of this see the cases of two cylinders and a cylinder plus a plane boundary in Table II.

3.8 THE EFFECT OF A NEARLY FREE SURFACE

Unlike the presence of a solid boundary, a free surface boundary adds considerably to the complexity of the problem. This is due to the fact that, in general, the boundary condition is non-linear and hence superposability is *not* satisfied. As a consequence the dynamic behavior of bodies near a free surface is a specialized area in which the literature is also rather specialized because of the complexity of the fluid flow problems. Though this subject is outside the scope of this report it is necessary to make a few brief remarks and, in particular, to identify the conditions under which one must account for free surface effects.

In the case of floating bodies the reader is referred to excellent reviews of the analytical techniques by Wehausen (Ref.12), Newman (Ref.13) and Oglvie (Ref.14). Submerged bodies are only slightly easier to handle. Some data on submerged bodies is given in Table III. It should be stressed that these examples are only pertinent to the inertial forces generated when accelerating the bodies *from rest*. Any prior translation or rotational motion of those bodies would have generated free surface waves which would in turn affect the unsteady loading on the body. This represents the major complication introduced by the presence of a free surface. It is however clear that if the body motion is sufficiently slow (characterized by a velocity, U, say) then the waves created will be negligibly small and these prior history effects would also be small. This requires that the Froude number, $U/(gd)^{\frac{1}{2}} << 1$.

The results of Table III do allow one to estimate what constitutes proximity to a free surface providing the above conditions hold. It can be seen that the free surface has little effect (less than 5%) provided the ratio of the depth of the body to the body dimension is greater than about 4. For lesser

CC BY

depths the added mass first increases as the acceleration of the fluid between the free surface and the body increases but then decreases when the depth is less than about one body dimension because less fluid is being accelerated.

3.9 THE EFFECT OF FLUID COMPRESSIBILITY

Generally the effects of the compressibility of the water on the added mass can be neglected in most ocean engineering applications. This is because the compressibility does not begin to affect the fluid flow until the Mach number ratio of the typical fluid velocity to the velocity of sound, c, in the fluid exceeds a value of at least 0.1. In unsteady flows one must also consider a parameter computed as the typical acceleration times the typical body dimension and divided by c. Again one would not normally expect any compressibility effect if this is less than 0.1.

Such conditions are almost always satisfied in ocean engineering applications. However it is possible that the presence of a large quantity of bubbles in the water could sufficiently reduce the sonic velocity, c, to such an extent that the added mass would be altered by the compresibility of the water/gas mixture.

CC BY

4. REVIEW OF EXISTING DATA ON ADDED MASS

4.1 THEORETICAL POTENTIAL FLOW ADDED MASSES

By far the largest category of analytical results for added mass are those calculated for bodies in an infinite fluid domain assuming the flow to be potential. The majority of these results are obtained by methods analogous to those described in Section 3. Bodies for which the steady flows can be generated by superposition of an array of potential flow singularities (sources, sinks, doublets, potential vortices, etc.) are particularly compatible with the use of expression (18). Such methods are described in Ref.9 and in many mechanics texts (e.g. Ref. 1, p.104). A particularly useful tabulation of many of the available results is given in a paper by Patton (Ref.8) and his Tables 1 and 2 are reproduced here as Tables I and III. Note that the third column of these tables contains the added mass denoted by m_h; the values given correspond to the diagonal terms in the added mass matrix, M_{ij}, the direction of acceleration being specified in the second column. (No off-diagonal components of the added mass matrix are listed.) Some results are also listed for bodies on or near to a solid or free surface and comment on these is delayed until later. Patton has included both theoretical potential flow added masses and experimentally determined added masses in Tables I and III. These are distinguished by the letters T and E in the fourth column of these tables. Another excellent source of tabulated added masses is given in a DTMB report by Kennard (Ref.9). Kennard's tables for added mass coefficients are attached to this report as Tables II, IV and V.

Though not exhaustive Tables I through IV provide a substantial reference list of added masses. It could be argued with some justification that these tables are more than adequate for most engineering purposes provided the body under analysis is not in close proximity to a solid or free surface. The remainder of this report will concentrate on the limitations of this analytical knowledge in terms of boundary effects and real fluid effects (e.g. viscous effects). However before proceeding to these discussions two further points should be made.

First Tables I through IV could be supplemented by the potential flow methods described in Section 3 and detailed in many references (e.g. Ref.9). Modern potential flow computer programs (e.g.Douglas-Neuman code) for *steady* flows could readily be adapted for this purpose as discussed in Section 3.5. The capability to do this might be important in circumstances where accurate added massses are required for bodies of unusual or complex geometry or in circumstances where the off-diagonal terms in the added mass matrix are deemed important (the tables contain virtually no information on off-diagonal terms).

The second point is that approximate values for the conventional or diagonal added mass terms for bodies of complex geometry (for example, an airplane) can be obtained by combining the added masses for each component of the structure (wings, fusilage, tail, etc). Such a strategy is outlined in Section 4.3.

4.2 SENSITIVITY TO THE GEOMETRY OF THE BODY

The diagonal terms in the added mass matrix (i.e. the conventional added masses) are relatively independent of the precise geometry of a body. For example, when accelerated normal to their longitudinal axes, cylinders with any elliptical cross-section have an added mass equal to that of a circular cylinder with the same width normal to the direction of acceleration under consideration (see Table I). Cylinders with more irregular rectangular or diamond shaped cross-sections deviate somewhat from this rule; however the deviations are rather unpredictable. Compare for example the fact that the rectangular and diamond shapes in Table I show opposite trends as the cross-section becomes more streamlined in the direction of acceleration. When the ratio of cross-sectional dimension in the direction of acceleration to that normal to the direction of acceleration is about 5 the rectangular shape has increased its added mass by a factor of 2 whereas the diamond shape has decreased its added mass by a factor of 40%. The unsubstantiated opinion of the author is that the experimental values would show less deviation due to the effects of flow separation.

Despite these deviations, a reasonable first approximation to the translational added mass, M_{ii}, for two dimensional bodies (large aspect ratio of length, l, to cross-sectional dimension, $2a_i$) would be the mass of a cylinder of fluid whose diameter is the same as the width, $2a_i$, of the projected area in the direction of acceleration, x_i:

CC BY

$$M_{ii} \approx \rho\pi(a_i)\, l \tag{25}$$

Consider therefore the following empirical approximation for arbitrary three dimensional bodies; that the added mass for a particular direction of acceleration, x_i, is given by the volume obtained by rotating the projected area of the body in that direction about an axis defined by the smaller of the two principal dimensions, $2a_i$, $2b_i$, of the projected area. For an elliptical projected area this would yield

$$M_{ii} = \frac{4}{3}\rho\pi b_i (a_i)^2, \quad b_i > a_i \tag{26}$$

where there is no implied summation over the index i. This would yield a reasonably conservative approximation for the preceding case of the cylinders. However it would substantially overestimate the added mass for a body like a sphere which has a small aspect ratio. Then the above estimate would be twice the potential flow value. Perhaps a better empirical approximation would be

$$M_{ii} = \frac{4}{3}\,\frac{\rho\pi(a_i)^2(b_i)^2}{(b_i + a_i)} \tag{27}$$

which would then predict both the cylinders and the sphere correctly. Testing this against the data for a prolate ellipsoid accelerating "broadside on" (see Table IV) we find a value of the added mass using Eq.(27) which is within 7% of the exact value. Further improvements could clearly be made but are probably of minor value considering the other uncertainties discussed below.

4.3 BODIES OF COMPLEX GEOMETRY

The result (27) of the previous section suggests an extension for the purposes of evaluating the added mass for a body of complex geometry (an airplane). Though it would require further detailed analysis and testing it would not be unreasonable to suggest that a complex body be considered disassembled into its principal component parts (wings, fuselage, tail) and that the added masses for each component be evaluated for three perpendicular directions of acceleration using the technique outlined in the previous section. Then we must ask whether it is approximately correct to simply add the added masses for the components in each of the three directions. From an engineering point of view it seems reasonable to do this. However it is very difficult to give any quantitative measure of the error in such an estimate due to the interaction of the components. The case of two parallel cylinders touching each other which is detailed in Table II, provides a particular harsh test. For directions parallel to and normal to the plane of the axes of the cylinders the errors would be 35.5% and 129% respectively. But this simply demonstrates that the two cylinders together should be treated as a single component; then the errors are significantly smaller namely 29% and 14% respectively.

Much more reasonable tests are provided by the winged objects in Table III and we shall, in particular examine the values given in Item 3, Table III. Taking the individual components (two flat plates and an ellipsoid) and using the tabulated added masses of these individual components in the case N=0.5 one arrives at a value of K of 1.293. This is within 5% of the actual value calculated namely 1.24.

Further tests would be needed to establish confidence limits on this superposition method but it does not seem unlikely that one could confidently predict potential flow added masses for complex bodies to within $\pm$ 30% using the methods outlined above and empirical formulae such as represented by Eq.(27).

4.4 THE EFFECTS OF A NEARLY SOLID BOUNDARY

The discussion in Sections 4.2 and 4.3 was confined to bodies remote from a solid boundary. It is clear from the various examples given in the tables that the presence of a solid boundary can cause substantial increase in the added mass. This is due to the necessary increase in the fluid accelerations primarily in the region between the fluid and the boundary. For example from Table II it is seen that the added mass for a circular cylinder (radius, a) is increased by a factor $a^2/2h^2$ for a wall at a distance h from the center of the cylinder. The result presented is only approximate and requires $a/h << 1$. If the body is brought closer to the boundary the added mass increases at an even greater rate because one develops a "film" or narrow gap between the body and the wall in which the fluid acceleration can be very large indeed.

From a practical engineering point of view there is a paucity of data for these extreme conditions of close proximity of a body to a solid boundary. A simple example will illustrate some of the dramatic effects of the proximity of a solid surface on the inertial forces required to move a body away from that surface. Consider the two dimensional problem of a flat plate of width, $2a$, lying on an ocean floor. A vertically upward force, F, per unit length of the plate is applied at the center of the plate to lift it away from the floor. Due to this force the plate has risen to a uniform height, $h(t)$, above the floor at time t. The velocity and acceleration of the plate in the upward direction are therefore dh/dt and d^2h/dt^2 (see Fig. 2).

Figure 2.

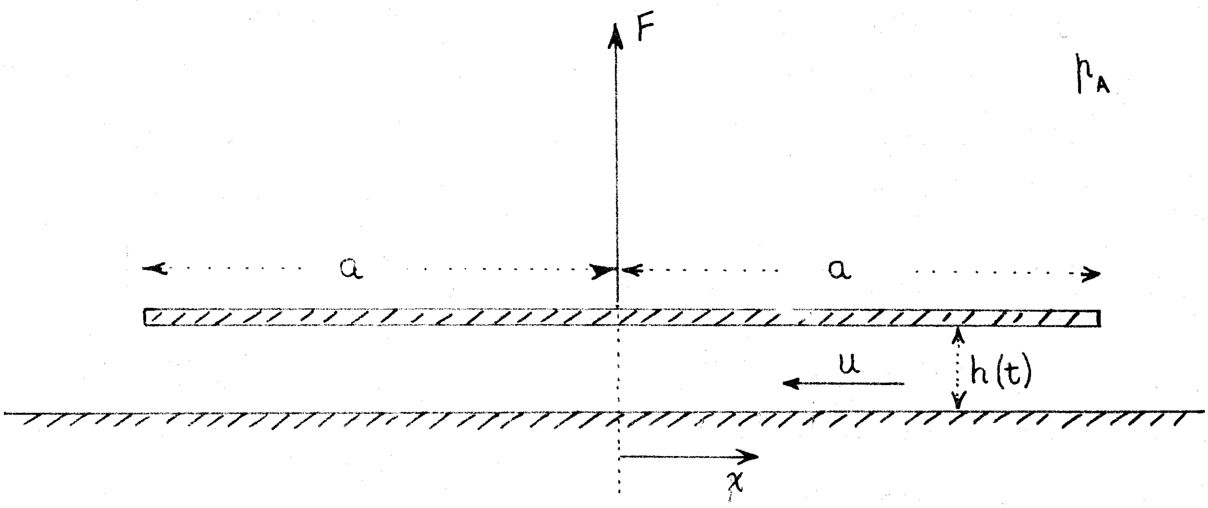

This problem could be visualized as characteristic of any fairly flat object lying on the ocean floor. Typically only portions of the undersurface would be in contact with the ocean floor. However one could visualize that prior to application of the force there is a typical average separation distance, h_0, between the undersurface and the object. Silting up of the object could, of course, make h_0 very small. In any case some h_0 would be pertinent to the moment, $t=0$, when the lift force is applied.

CC BY

We concentrate here on the dynamics of the body while the separation, h is very small compared with the lateral dimension, $2a$, of the object because it will be seen that these are the most critical conditions. Then upward velocity of the plate, dh/dt, will generate much larger horizontal velocities, u, (Fig.2), in the gap than vertical velocities and hence continuity of mass in the gap requires

$$h\,u = -\frac{dh}{dt}x \tag{28}$$

and the momentum equation for the fluid in the gap in the absence of frictional or viscous forces yields

$$\frac{1}{\rho}\frac{\partial p}{\partial x} + 2u\frac{\partial u}{\partial x} + \frac{1}{h}\frac{\partial}{\partial t}(hu) = 0 \tag{29}$$

where $p(x,t)$ pressure at any point, x, in the gap. Substitution and integration yield the following form for the pressure distribution in the gap

$$p = p_E + \frac{\rho}{2}(a^2 - x^2)\,h\,\frac{\partial^2}{\partial t^2}\left[\frac{1}{h}\right] \tag{30}$$

where p_E is the pressure at the edges, $x = \pm a$. While the gap is small p_E will be approximately equal to the ambient pressure, p_A, and the pressure on the top-side will deviate much less from p_A than the pressure p in the gap. Consequently by integration using the relation for p, one can obtain the downward inertial force or added mass force, F, imposed by the fluid on the plate (per unit plate length)

$$F = \frac{2}{3}\rho\,\frac{a^3}{h}\left\{\frac{\partial^2 h}{\partial t^2} - \frac{2}{h}\left[\frac{\partial h}{\partial t}\right]^2\right\} \tag{31}$$

Compare this with the known inertial force on the plate in the absence of the solid boundary namely $\rho\pi a^2\,\partial^2 h/\partial t^2$ where $\partial^2 h/\partial t^2$ is again used to represent the vertically upward acceleration. It is clear that the magnitude of the former given by Eq.(31) will typically be very much larger than the latter by the large factor, a/h. Of course the preceding analysis ceases to be valid when h approaches a. But it is clear that as the plate is raised the added mass per unit length begins at a very large value of the order of $\rho a^3/h_0$ and will rapidly decrease with h so that it asymptotically approaches a value of the order of ρa^2 when h is of the order a.

CC BY

It is of interest to examine briefly the consequences of this behavior of the fluid inertial forces. If, for simplicity one neglects the mass of the plate itself, then the upward force applied to the plate by the cable will be equal and opposite to the fluid inertial force. For illustrative purpose suppose a constant upward cable force is applied. Then integration of the equation of motion represented by Eq.(31) if F is now visualized as the cable force yields a time history $h(t)$, given by

$$h=\frac{h_0}{\cos\lambda t} \quad ; \quad \lambda=\left[\frac{3F}{2\rho a^3}\right]^{\frac{1}{2}} \tag{32}$$

where the initial conditions $h=h_0$ and $dh/dt=0$ at $t=0$ have been used. It is readily seen that this leads to a kind of "catastrophic" release from the bottom in which the upward acceleration increases with time. It is unlikely therefore that a constant uplift force could be maintained under these circumstances. Consequently the actual initial motion would be dependent on other factors such as the cable elasticity.

The author has, as yet, encountered little in the way of analysis of such problems and suggests this as an area deserving further study both experimentally and analytically.

4.5 VISCOUS EFFECTS ON ADDED MASS AND DRAG

The previous sections of this chapter have deliberately avoided reference to a further complication caused by the viscous effects in the flow around the body. These viscous effects on both the fluid inertial and fluid drag forces have been the subject of a number of detailed studies as represented for example by Refs.10, 11 and 15. The essence of the complication is that in certain regimes of flow the viscous processes of flow separation and vortex shedding cause radical modifications to the forces expected on the basis of simple addition of fluid inertial and fluid drag forces. The latter approximation is embodied in what is known as Morison's equation (Ref.16) in which the total force on the body, F^T, is expressed as

$$F_i^T=-M_{ij}\frac{dU_j}{dt}-\frac{1}{2}\rho AC_{ij}\left\{\left[U_j\right]\right\}^2 \tag{33}$$

where C_{ij} is a lift and drag coefficient matrix, and A is a typical area for the body. This equation is

CC BY

normally quoted for only one direction at a time and is written as

$$F^T = -M \frac{dU}{dt} - \frac{1}{2}\rho A C_D |U|^2 \tag{34}$$

where C_D, U and dU/dt refer to a drag coefficient, the velocity and acceleration in line with the force. It might be expected that both M and C_D would be independent of the specific motion under consideration. However Keulegan and Carpenter (Ref.10) have observed experimentally that this was not the case and that substantial changes in M and C_D occurred as the rate of acceleration represented by the period, T, of their sinusoidal motion was increased such that $U_M T/D$ became of order one. Here U_M is the typical velocity (the peak velocity of the sinusoidal motion) and D is the cylinder or plate width. It is significant that all of their data was obtained within a range of Reynolds numbers, $U_M D/\nu$ (ν is the kinematic viscosity) between 5000 and 30,000. Even the steady flows past bodies in this Reynolds number regime experience substantial unsteadiness due to flow separation and vortex shedding.

Keulegan and Carpenter found that the "effective" value of the added mass for cylinders was close to the potential flow value ($\rho\pi D^2/4$ per unit length) for $U_M T/D$ below about 5 but decreased rapidly with increasing $U_M T/D$ becoming negative for a range of $U_M T/D$ between 10 and 20! (Note that we have subtracted the displaced fluid mass from their results to get the true added mass in line with the discussion of Section 3.6.) With further increase in $U_M T/D$ positive values similar to those for $U_M T/D < 5$ are recovered. The drag coefficient, C_D, shows a large increase for the same range of $U_M T/D$ betweeen 10 and 20. Flat plates exhibited a different pathological behavior of the added mass and drag coefficient. No systematic variations with Reynolds number, $U_M D/\nu$, could be detected.

Skop, Ramberg and Ferer (Ref.15) have also carried out experiments on sinusoidally oscillating flows except that the body rather than the fluid is accelerated. Their results do not agree with those of Keulegan and Carpenter. For values of $U_M T/D$ between 1 and 12 they found that the fluid inertial force agreed very well with the potential flow value. Moreover the variations in the effective drag coefficient could be accurately predicted by considering the instantaneous Reynolds number at each point during the cycle, using some appropriate form for the corresponding instantaneous drag and

CC BY

thereby synthesizing the overall drag coefficient.

The results of Skop, Ramberg and Ferer cannot be readily reconciled with those of Keulegan and Carpenter. The Reynolds numbers for the Skop, Ramberg and Ferer experiments are in the range between 230 and 40,000 and are therefore similar to those of Keulegan and Carpenter. It is quite clear that further detailed measurements using more sophisticated measurement and data analysis techniques are needed to resolve this question. Though it has little value, I have formed the very tentative opinion that the experiments and data reduction techniques used by Skop, Ramberg and Ferer are superior to those of Keulegan and Carpenter and therefore I would place more confidence in their results. On the other hand the data of Keulegan and Carpenter is much more widely known and used; this I believe may be unfortunate.

For the present it is necessary for engineering purposes to be aware that pathological behavior of the fluid inertial forces *might* occur for body motions whose typical amplitude is greater than about half of the body dimension.

Before leaving this subject it is of value to Secord a few of the results of the experiments carried out by Sarpkaya (Ref.11). He oscillated a cylinder in a direction normal to the direction of an oncoming stream of fluid and observed pathological behavior for $\bar{V}T/D$ (where $\bar{V}$ is now the steady stream velocity) between about 3 and 10. Furthermore, in one of the few experimental measurements of off-diagonal terms in the force matrix he observed the oscillations in the force on the body perpendicular to the direction of oscillatory motion to be less than 7% of the steady drag in that direction.

CC BY

5. SUMMARY

The analytical background of the added mass matrix describing fluid forces due to acceleration of the body or the fluid has been reviewed. It is shown that the use of this concept is rigorously justified only in the case of linearly superposable fluid motions with rigid boundaries. In the context of ocean engineering problems this restricts the analysis to that of potential flow and, indeed, almost all of the theoretical predictions are computed from potential flow analysis. For empirical engineering purposes the concept has also been used for real flows with boundary layers, separation and vortex shedding.

The majority of potential flow calculations of added mass are for bodies accelerated in an infinite domain of incompressible, inviscid fluid. Many of these are included in Tables I to IV. These tables provide a substantial reference list which may be more than adequate for many engineering purposes provided the body is not in close proximity to a solid or free surface boundary. Furthermore since the added mass is generally rather insensitive to the detailed geometry of the body we have some preliminary suggestions as to how the added mass for a body of complex geometry might be estimated. As detailed in Sections 4.2 and 4.3 the first step is to decompose the body into major components. The added mass of each may then be estimated for each direction of acceleration from the principal dimensions ($2a_i$, $2b_i$) of the projected area in that direction and the approximate formula (27). The added mass for each component in each direction would then be arithmetically summed. I believe it might be possible to make predictions within ± 30% by this means. If better accuracy is required then we have indicated how modern potential flow codes (.e.g Douglas-Neuman code) designed to calculate steady flows might be utilized to obtain better results.

Data is scarcer for the cases when a solid boundary or free surface is close to the body. In general modifications are required if such a boundary is within four major body dimensions. Free surface effects are quite complex and are not covered by this report. However it is shown that a solid surface (ocean bed) can have a dramatic effect particularly when a body is being raised from the ocean floor.

Data is also scarce for the off-diagonal elements of the added mass matrix. Virtually no results for these elements appear in the tables. Consequently it is almost impossible to assess whether these interaction terms are important in practical problems. Again, however, use of the aforementioned computer codes would permit better evaluation of the need to consider the off-diagonal terms.

The relationship between the forces when the fluid is accelerating past the body as opposed to the reverse is discussed in Section 3.6. It is shown that a relation can only be firmly established if either (i) superposability is possible (e.g. potential flow) or (ii) if the entire previous history of the relative velocity is identical in the two cases. Then the appropriate fluid mass in the case of fluid acceleration is equal to the added mass plus the displaced fluid mass.

Finally it is clear that viscous effects in the form of boundary layer separation and particularly vortex shedding could possibly cause radical departures from the theoretical, potential flow predictions. The data on this is limited and contradictory. For the present one can only point out that pathological behavior *might* occur in certain ranges of frequency (or typical time of acceleration) and Reynolds number.

6. RECOMMENDATIONS

It seems appropriate to suggest several areas of engineering importance in which further analytical, empirical and experimental studies would provide valuable information.

A. There is a relative paucity of good experimental data in the open literature which can be used to evaluate the real fluid effects of viscosity. The data which does exist is often contradictory. Such experiments are not easy and are frought with pitfalls. However both measurement techniques and data processing methods have substantially improved in the last five years. It therefore seems appropriate to suggest further experimental programs which might help to provide some solid information that the engineer could use. At the present time there is little concrete knowledge which the engineer could use with confidence.

B. The theoretical predictions of added mass from potential flow provide a good data base for use in estimating the diagonal terms in the added mass matrix. This data base would be utilized to produce empirical methods for use with bodies of complex geometry. This could result in a simple and useful computer code for this purpose.

C. There are however very few calculated values for the off-diagonal terms in added mass matrices. I therefore recommend that in order to build up some data base for off-diagonal terms *and* in order to allow more accurate evaluation of the diagonal terms for bodies of complex geometry some of the modern potential flow computer codes (e.g. Douglas-Neuman) be adapted to evaluate the entire added mass matrix.

D. The dramatic effects which can occur during separation of a body from the ocean floor should be further investigated both analytically and experimentally.

7. REFERENCES

1. Yih, C-S. 1969. Fluid Mechanics. McGraw-Hill Book Co.
2. Lamb, H. 1932. Hydrodynamics, Dover Pub., 6th Edition.
3. Birkhoff, G. 1960. Hydrodynamics, Princeton Univ. Press.
4. Munk, M. 1963. Fluid Mechanics, Part II, Aerodynamic Theory, Vol.1 edited by W.Durand, Dover Pub., NY.
5. Patton, K.t. 1965. Tables of hydrodynamic mass factors for translational motion. ASME Paper, 65-WA/UNT-2.
6. Wendel, K. 19 . Hydrodynamic masses and hydrodynamic moments of inertia, DTMB Translation, No.260. Kinsler, L.E. and Frey, A.R. 1962. Fundamentals of Acoustics, J.Wiley and Sons, NY.
7. Patton, K.T. 1965. An experimental investigation of hydrodynamic mass and mechanical impedances. MS Thesis, Univ. of Rhode Island.
8. Kennard, E.M. 1967. Irrotational flow of frictionless fluid, mostly of invariable density. DTMB Report 2299.
9. Keulegan, G.H. and Carpenter, L.H. 1958. Forces on cylinders and plates in an oscillating fluid. J.Res.Nat.Bur.Standards, Vol.60, No.5, pp.423-440.
10. Sarpkaya, T. 1977. Transverse oscillation of a circular cylinder in uniform flow. Naval Postgraduate School, Monterey, Report NPS-69SL77071-R.
11. Wehausen, J.V. 1971. Motion of floating bodies. Ann. Rev.Fluid Mech., Vol.3, pp.237-268.
12. Newman, J.N. 1970. Ann. Rev.Fluid Mech., Vol.2, pp.67-94.
13. Ogilvie, T.F. 1964. Recent progress toward the understanding and prediction of ship motions. 5th Symp.Naval Hydrodynamics, Bergen, pp.3-128.
14. Skop, R.A., Ramberg, S.E. and Ferer, K.M. 1976. Added mass and damping forces on circular cylinders. Naval Research Laboratory, Washington, D.C., Report NRL 7970.

BY

15. Morison, J.R., O'Brien, M.P., Johnson, J.W. and Schaaf, S.A. The forces exerted by surface waves on piles. J.Petrol.Tech., A.I.M.E., Vol.189, p.149.

16. Sarpkaya, T. and Isaacson, M. 1981. Mechanics of wave forces on offshore structures. Van Nostrand Reinhold Co., New York.

17. Blevins, R.D. 1977. Flow-induced vibrations. Van Nostrand Reinhold Co., New York.

TABLE I

(From Reference 5)

ADDED (HYDRODYNAMIC) MASSES FOR TWO-DIMENSIONAL POTENTIAL FLOWS ; Reference numbers are given under SOURCE.

SECTION THROUGH BODY	TRANSLATIONAL DIRECTION	HYDRODYNAMIC MASS PER UNIT LENGTH	SOURCE
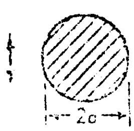	Vertical	$m_h = 1\,\pi\rho a^2$	6 T
	Vertical	$m_h = 1\,\pi\rho a^2$	6 T
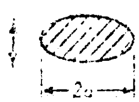	Vertical	$m_h = 1\,\pi\rho a^2$	6 T
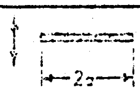	Vertical	$m_h = 1\,\pi\rho a^2$	6,8 T,E
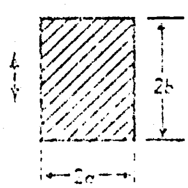 $a/b = \infty$	Vertical	$m_h = 1\,\pi\rho a^2$	6 T
$a/b = 10$		$m_h = 1.14\,\pi\rho a^2$	6 T
$a/b = 5$		$m_h = 1.21\,\pi\rho a^2$	6 T
$a/b = 2$		$m_h = 1.36\,\pi\rho a^2$	6 T
$a/b = 1$		$m_h = 1.51\,\pi\rho a^2$	6 T
$a/b = 1/2$		$m_h = 1.70\,\pi\rho a^2$	6 T
$a/b = 1/5$		$m_h = 1.98\,\pi\rho a^2$	6 T
$a/b = 1/10$		$m_h = 2.23\,\pi\rho a^2$	6 T
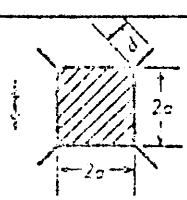 $d/a = .05$	Vertical	$m_h = 1.61\,\pi\rho a^2$	6 T
$d/a = .10$		$m_h = 1.72\,\pi\rho a^2$	6 T
$d/a = .25$		$m_h = 2.19\,\pi\rho a^2$	6 T

TABLE I (continued)

SECTION THROUGH BODY	TRANSLATIONAL DIRECTION	HYDRODYNAMIC MASS PER UNIT LENGTH	SOURCE
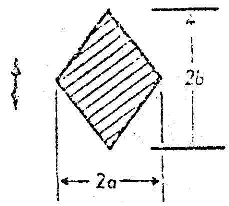 a/b = 2	Vertical	$m_h = .85 \pi \rho a^2$	6 T
a/b = 1		$m_h = .76 \pi \rho a^2$	6 T
a/b = 1/2		$m_h = .67 \pi \rho a^2$	6 T
a/b = 1/5		$m_h = .61 \pi \rho a^2$	6 T
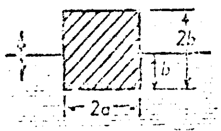 a/b = 1	Vertical (normal to free surface)	$m_h = .75 \pi \rho a^2$	6 T
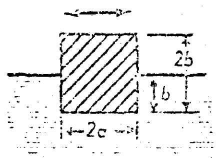 a/b = 1	Horizontal (parallel to free surface)	$m_h = .25 \pi \rho a^2$	6 T
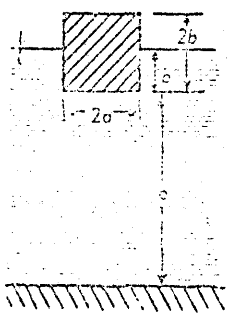 a/b = 1; c/b = ∞	Vertical (normal to free surface)	$m_h = .75 \pi \rho a^2$	6 T
c/b = 2.6		$m_h = .83 \pi \rho a^2$	6 T
c/b = 1.8		$m_h = .89 \pi \rho a^2$	6 T
c/b = 1.5		$m_h = 1.00 \pi \rho a^2$	6 T
c/b = .5		$m_h = 1.35 \pi \rho a^2$	6 T
c/b = .25		$m_h = 2.00 \pi \rho a^2$	6 T
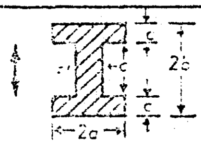 a/c = 2.6, b/c = 3.6	Vertical	$m_h = 2.11 \pi \rho a^2$	8 E

CC BY

TABLE II
(From Reference 9)

ADDED MASSES FOR TWO-DIMENSIONAL POTENTIAL FLOWS
(See Reference 9 or TABLE V for notation)

Circular cylinder in translation perpendicular to its axis:

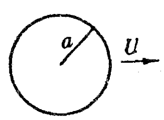

$$T_1 = \frac{1}{2} \rho\pi \; a^2 U^2, \qquad \text{as in Equation [68i],}$$

$$M_1' = \rho\pi \; a^2, \qquad k = 1.$$

Elliptic cylinder in translation parallel to an axis, called the a-axis, either $a > b$ as shown or $b > a$:

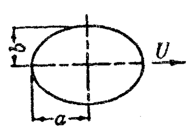

$$T_1 = \frac{1}{2} \rho\pi \; b^2 U^2, \qquad \text{from Equation [84l],}$$

$$M_1' = \rho\pi \; ab, \qquad k = b/a.$$

Plane lamina in translation perpendicular to its faces:

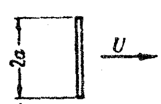

$$T_1 = \frac{1}{2} \rho\pi \; a^2 U^2, \qquad \text{as in Equation [86b],}$$

$$kM_1' = \rho\pi \; a^2.$$

Elliptic cylinder rotating about its axis:

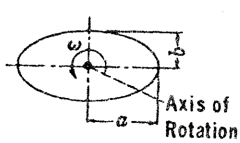

$$T_1 = \frac{1}{16} \rho\pi (a^2 - b^2)^2 \; \omega^2, \qquad \text{as in Equation [106z],}$$

$$I_1 = \frac{1}{4} \rho\pi \; ab(a^2 + b^2), \qquad k = \frac{(a^2 - b^2)^2}{2ab\,(a^2 + b^2)}.$$

Plane lamina rotating about its central axis:

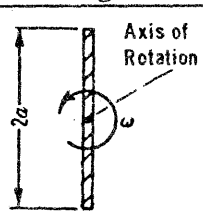

$$T_1 = \frac{1}{16} \rho\pi \; a^4 \omega^2, \qquad \text{as in Equation [106a']},$$

$$kI_1' = \frac{1}{8} \rho\pi \; a^4.$$

TABLE II (continued)

Plane lamina rotating about one edge:

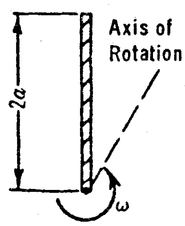

$$T_1 = \frac{9}{16}\rho\pi\ a^4\omega^2,$$ as in Equation [106b′] with $\beta = 1$,

$$\frac{\text{Apparent increase in moment of inertia}}{\text{Moment of inertia of fluid displaced by a cylinder of radius } a \text{ rotating as if rigid about a generator}} = \frac{9\rho\pi\ a^4/8}{3\rho\pi\ a^4/2} = \frac{3}{4}$$

Fluid inside elliptic-cylindrical shell rotating about its axis:

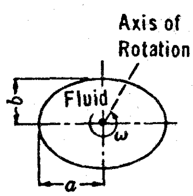

$$T_1 = \frac{1}{8}\rho\pi ab\frac{(a^2-b^2)^2}{a^2+b^2}\omega^2,$$ as in Equation [105m],

$$I_1' = \frac{1}{8}\rho\pi ab\,(a^2+b^2), \qquad k = \left(\frac{a^2-b^2}{a^2+b^2}\right)^2.$$

Fluid inside semicircular cylindrical shell rotating about axis of the semicircle

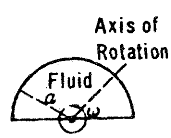

$$T_1 = \frac{\pi}{4}\left(\frac{8}{\pi^2}-\frac{1}{2}\right)\rho a^4\omega^2,$$ as in Equation [102e],

$$I_1' = \frac{\pi}{4}\rho a^4, \qquad k = 2\left(\frac{8}{\pi^2}-\frac{1}{2}\right) = 0.621.$$

Fluid inside equilateral triangular prism rotating about its central axis:

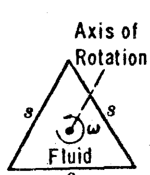

$$T_1 = \frac{1}{80\sqrt{3}}\rho s^4\omega^2,$$ as in Equation [103k],

$$I_1' = \frac{1}{16\sqrt{3}}\rho s^4, \qquad k = \frac{2}{5}.$$

Lamina bent in form of circular arc, in translation at angle θ with chord:

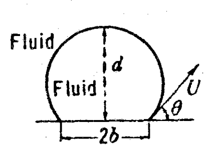

$$T_1 = \frac{1}{2}\rho\pi\left(b^2\sin^2\theta + \frac{d^2}{2}\right)U^2,$$ as in Equation [78r].

cc BY

TABLE II (continued)

Cylinder with contour consisting of two similar circular arcs; see Section 89.

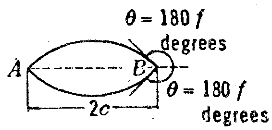

Cross-sectional area $S = \dfrac{c^2}{\sin^2\theta}\left[2(1-f)\,\pi + \sin 2\,\theta\right]$

1. Translation parallel to chord AB. $T_1 = \dfrac{1}{2}\rho k\,SU^2$, $\quad k = \dfrac{2\pi}{3}\left(\dfrac{1}{f^2} - 1\right)\dfrac{c^2}{S} - 1.$

2. Translation perpendicular to chord AB: $T_1 = \dfrac{1}{2}\rho k\,SU^2$, $\quad k = \dfrac{2\pi}{3}\left(\dfrac{1}{2f^2} + 1\right)\dfrac{c^2}{S} - 1.$

Cylinder with contour formed by two similar parabolic arcs meeting perpendicularly; see Section 91(d):

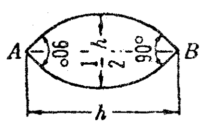

$M_1' = \dfrac{1}{3}\rho h^2$, $\quad T_1 = \dfrac{1}{2}kM_1'U^2$;

1. Translation parallel to chord AB: $k = \dfrac{4K^4}{\pi^3} - 1 = 0.525.$

2. Translation perpendicular to chord AB: $k = \dfrac{8K^4}{\pi^3} - 1 = 2.049.$

Here $K = 1.8541$, the complete elliptic integral of modulus $\sqrt{1/2}$.

Cylinder whose contour is formed by four equal semicircles:

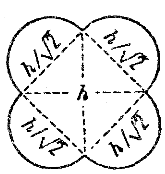

$M_1 = \dfrac{1}{4}(2+\pi)\,\rho h^2$; $\quad$ for translation in any direction

$T_1 = \dfrac{1}{2}kM_1U^2$, $\quad k = \dfrac{\pi}{2+\pi}K^2 - 1 = 1.100.$

For K, see the preceding case. See Section 91(e).

Double circular cylinder, each cylinder of radius a; see Section 90:

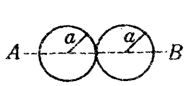

$M_1' = 2\rho\pi a^2.$

1. Translation parallel to line of axes AB: $T_1 = \rho\pi a^2U^2\left(\dfrac{\pi^2}{6} - 1\right)$, $\quad k = \dfrac{\pi^2}{6} - 1 = 0.645.$

2. Translation perpendicular to line of axes AB: $T_1 = \rho\pi a^2U^2\left(\dfrac{\pi^2}{3} - 1\right)$, $\quad k = \dfrac{\pi^2}{3} - 1 = 2.290.$

cc BY

TABLE II (continued)

Cylinder of radius a sliding along fixed plane wall; see Section 90.

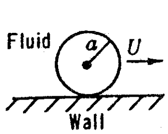

$$T_1 = \frac{1}{2}\rho\pi a^2 U^2\left(\frac{\pi^2}{3} - 1\right).$$

$$M_1' = \rho\pi a^2, \qquad k = \frac{\pi^2}{3} - 1 = 2.290.$$

Cylinder of rhombic cross-section, in translation along a diagonal; see Section 91(c).

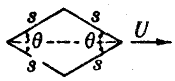

$$M_1' = \rho\, s^2 \sin\theta$$

$$T_1 = \frac{1}{2} k M_1 U^2, \qquad k = \frac{2\theta}{\sin\theta}\,\frac{\Gamma(3/2)}{\Gamma\left(1 - \frac{\theta}{2\pi}\right)\Gamma\left(\frac{1}{2} + \frac{\theta}{2\pi}\right)} - 1.$$

Here θ is in radians and Γ stands for the gamma function.

Rectangular cylinder in translation parallel to a side; see Section 91(b) for references.

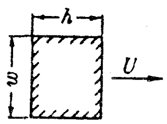

$M_1'' = k M_1' =$ apparent increase in mass,

$M_{10}'' = \rho\pi w^2/4$ or M_1'' for a plane lamina of width w.

$h/w =$	0	0.025	0.111	0.298	0.676	1.478	3.555	9.007	40.03
$M_1''/M_{10}'' =$	1	1.05	1.16	1.29	1.42	1.65	2.00	2.50	3.50

Circular cylinder with symmetrical fins:

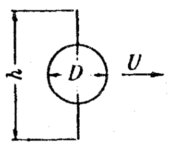

$$T_1 = \frac{1}{2} k M_1 U^2, \qquad \text{as in Equation [91g]},$$

$$M_1' = \frac{1}{4}\rho\pi D^2, \qquad k = 1 + \left(\frac{h}{D} - \frac{D}{h}\right)^2.$$

Cylinder of radius a in translation and instantaneously coaxial with enclosing fixed cylinder of radius b:

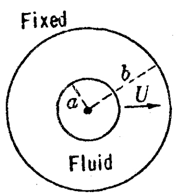

$$T_1 = \frac{1}{2}\rho\pi a^2 U^2\,\frac{b^2 + a^2}{b^2 - a^2}, \qquad \text{as in Equation [104f]}$$

$$M_1' = \rho\pi a^2, \qquad k = \frac{b^2 + a^2}{b^2 - a^2}.$$

TABLE II (continued)

Cylinder of radius a in translation in any direction across axis of enclosing fixed square cylinder of side s, a/s small; see Section 91(1).

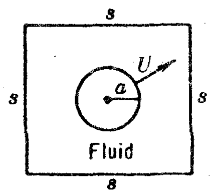

$$T_1 = \frac{1}{2}\rho\pi a^2 U^2 \left(1 + 6.88\frac{a^2}{s^2} \ldots\right),$$

$$M_1' = \rho\pi a^2, \qquad k = 1 + 6.88\frac{a^2}{s^2} \ldots$$

Cylinder of radius a in translation in any direction near a fixed infinite wall, a/h small:

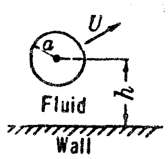

$$T_1 = \frac{1}{2}\rho\pi a^2 U^2 \left(1 + \frac{a^2}{2h^2} \ldots\right), \qquad \text{as in Equation [95g]}$$

$$M_1' = \rho\pi a^2, \qquad k = 1 + \frac{a^2}{2h^2} + \ldots$$

(Only the force required to accelerate the cylinder is considered here.)

Cylinder of radius a moving symmetrically between fixed infinite walls h apart, a/h rather small:

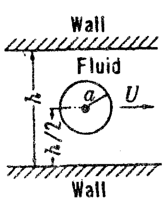

$$T_1 = \frac{1}{2}\rho\pi a^2 U^2 \left[1 + \frac{2}{3}\left(\frac{\pi a}{h}\right)^2 + \ldots\right], \qquad \text{as in Equation [46q]}$$

$$M_1 = \rho\pi a^2, \qquad k = 1 + \frac{2}{3}\,\frac{\pi^2 a^2}{h^2} \ldots$$

Plane lamina of width b moving symmetrically between fixed infinite rigid walls h apart, b/h rather small:

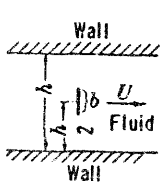

$$T_1 = \frac{1}{2}\rho U^2 \frac{\pi b^2}{4}\left(1 + \frac{\pi^2 b^2}{24h^2} \ldots\right), \qquad \text{as in Equation [65l]}$$

TABLE III

(From Reference 5)

ADDED MASSES FOR THREE-DIMENSIONAL POTENTIAL FLOWS
Reference numbers are given under SOURCE.

BODY SHAPE	TRANSLATIONAL DIRECTION	HYDRODYNAMIC MASS	SOURCE
1. *FLAT PLATES* *Circular Disc* 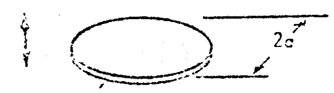	Vertical	$m_h = \frac{8}{3} \rho a^3$ Effect of Frequency of Oscillation on Hydrodynamic Mass of a Circular Disc 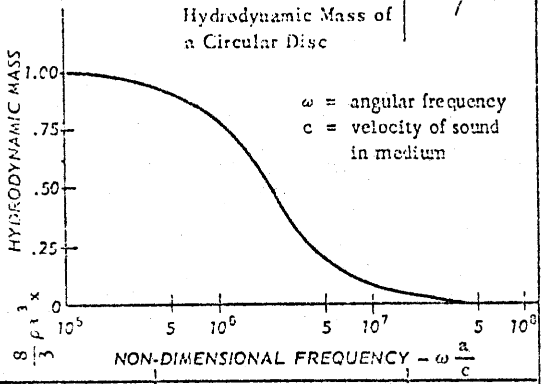	T 2,7 7
Elliptical Disc 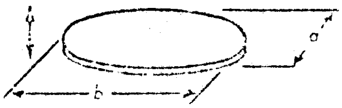	As Shown	$m_h = Kba^2 \frac{\pi}{6} \rho$ b/a — K ∾ — 1.00 14.3 — .991 12.75 — .987 10.43 — .985 9.57 — .983 8.19 — .978 7.00 — .972 6.00 — .964 5.02 — .952 4.00 — .933 3.00 — .900 2.00 — .826 1.50 — .748 1.00 — .637	4 T
Rectangular Plates 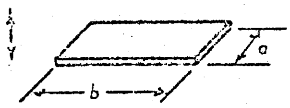	Vertical	$m_h = K \pi \rho \frac{a^2}{4} b$ b/a — K 1.0 — .478 1.5 — .680 2.0 — .840 2.5 — .953 3.0 — 1.00 3.5 — 1.00 4.0 — 1.00 ∾ — 1.00	8 E

CC BY

TABLE III (continued)

BODY SHAPE	TRANSLATIONAL DIRECTION	HYDRODYNAMIC MASS	SOURCE
Triangular Plates 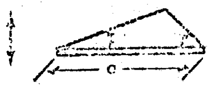 	Vertical	$m_h = \frac{\rho}{3} a^3 \frac{(\mathrm{TAN}\ \theta)^{3/2}}{(\pi)}$	8 E
2. *BODIES OF REVOLUTION* *Spheres* 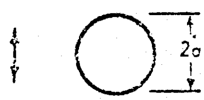 	Vertical	$m_h = \frac{2}{3} \pi \rho a^3$	1,2 T
Ellipsoids 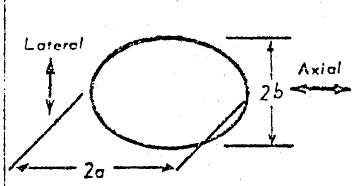 	Vertical a/b 1.00 1.50 2.00 2.51 2.99 3.99 4.99 6.01 6.97 8.01 9.02 9.97	$m_h = K \cdot \frac{4}{3} \pi \rho a b^2$ K for Axial Motion / K for Lateral Motion .500 / .500 .305 / .621 .209 / .702 .156 / .763 .122 / .803 .082 / .860 .059 / .895 .045 / .918 .036 / .933 .029 / .945 .024 / .954 .021 / .960 0 / 1.000	2 T

CC BY

TABLE III (continued)

BODY SHAPE	TRANSLATIONAL DIRECTION	HYDRODYNAMIC MASS	SOURCE

Approximate Method for Elongated Bodies of Revolution.

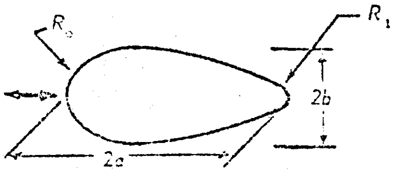

4

$$m_h = K_1 \rho V = Ke\left[1 + 17.0\left(Cp - \frac{2}{3}\right)^2 + 2.49\left(M - \frac{1}{2}\right)^2 + .283\left[\left(r_o - \frac{1}{2}\right)^2 + \left(r_1 - \frac{1}{2}\right)^2\right]\right]$$

where; K_1 – Hydrodynamic Mass coefficient for axial motion

K_e – Hydrodynamic Mass coefficient for axial motion of an ellipsoid of the same ratio of a/b

V - Volume of body

C_p – Prismatic coefficient $= \dfrac{4V}{b^2(2a)}$

M – Nondimensional abscissa $\dfrac{X_m}{l}$ corresponding to maximum ordinate

r_o, r_1 – Dimensionless radii of curvature at nose and tail

$$r_o = \frac{Ro(2a)}{b^2} \qquad r_1 = \frac{R1(2a)}{b^2}$$

E

	Lateral Motion	Munk has shown that the hydrodynamic mass of an elongated body of revolution can be reasonably approximated by the product of the density of the fluid, the volume of the body and the k - factor for an ellipsoid of the same a/b ratio.	4

TABLE III (continued)

BODY SHAPE	TRANSLATIONAL DIRECTION	HYDRODYNAMIC MASS	SOURCE
Sphere Near a Free Surface 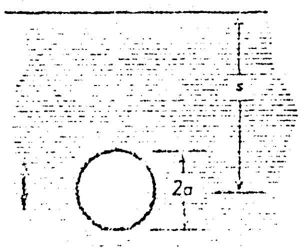	Vertical	$m_h = K \cdot \frac{4}{3}\pi\rho a^3$ $s/2a$ — K 0 — .50 .5 — .88 1.0 — 1.08 1.5 — 1.16 2.0 — 1.18 2.5 — 1.18 3.0 — 1.16 3.5 — 1.12 4.0 — 1.04 4.5 — 1.00	8 E
Ellipsoid Near a Free Surface 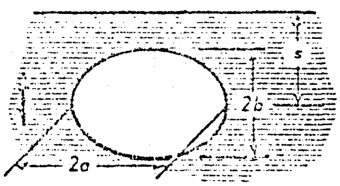	Vertical	$m_h = K \cdot \frac{4}{3}\pi\rho ab^2$ $a/b = 2.00$ $s/2b$ — K 1.00 — .913 2.00 — .905	8 E
3. *BODIES OF ARBITRARY SHAPE* *Ellipsoid with Attached Rectangular Flat Plates* 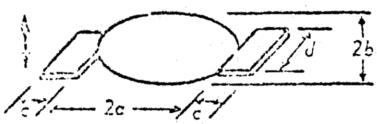	Vertical	$m_h = K \cdot \frac{4}{3}\pi\rho ab^2$ $a/b = 2.00;\ c = b$ $c.d = N\pi ab$ N — K 0 — .7024 .20 — .8150 .30 — 1.0240 .40 — 1.1500 .50 — 1.2370	8 E
Ellipsoid with Attached Rectangular Flat Plates Near a Free Surface 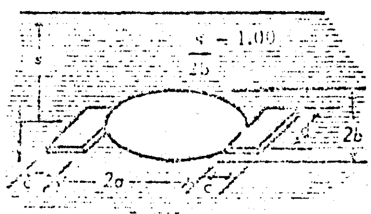	Vertical	$m_h = K \cdot \frac{4}{3}\pi\rho ab^2$ $a/b = 2.00;\ c = b$ $c.d = N\pi ab$ N — K 0 — .9130 .20 — 1.0354 .30 — 1.3010 .40 — 1.4610 .50 — 1.5706	8 E

CC BY

TABLE III (continued)

BODY SHAPE	TRANSLATIONAL DIRECTION	HYDRODYNAMIC MASS	SOURCE
Streamlined Body 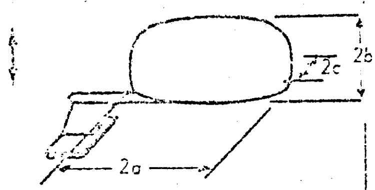 $\frac{a}{b} = 2.38$ $\frac{a}{c} = 2.11$ Area of Horizontal "Tail" – 25% of Area of Body Maximum Horizontal Section.	Vertical	$m_h = 1.124\,\rho\left[\frac{4}{3}\pi a d^2\right]$ $d = \frac{c+b}{2}$	8 E
Streamlined Body 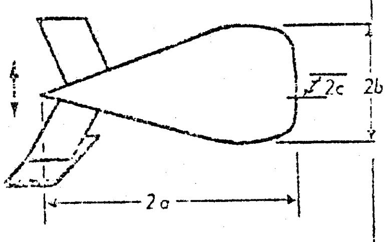 $\frac{a}{b} = 2.4$ $\frac{a}{c} = 3.0$ Area of Horizontal "Tail" – 20% of Area of Body Maximum Horizontal Section.	Vertical	$m_h = .672\,\rho\left[\frac{4}{3}\pi a d^2\right]$ $d = \frac{c+b}{2}$	8 E
"Torpedo" Type Body 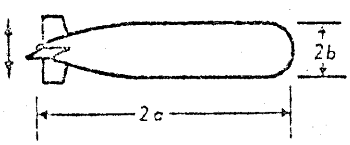 $\frac{a}{b} = 5.0$ Area of Horizontal "Tail" = 10% of Area of Body Maximum Horizontal Section.	Vertical	$m_h = .818\,\pi\,\rho\,b^2(2a)$	8 E

TABLE III (continued)

BODY SHAPE	TRANSLATIONAL DIRECTION	HYDRODYNAMIC MASS	SOURCE
V-Fin Type Body 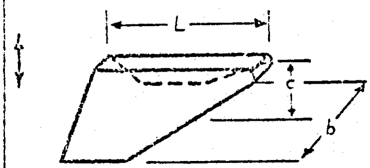 $\frac{L}{b} = 1.0$ $\frac{L}{c} = 2.0$	Vertical	$m_h = .3975\,\rho\,L^3$	8 E
Parallelepipeds 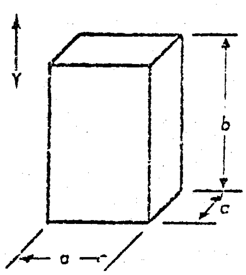	Vertical	$m_h = K\,\rho\,a^2 b$ b/a — K 1 — 2.32 2 — .86 3 — .62 4 — .47 5 — .37 6 — .29 7 — .22 10 — .10	8 E

CC BY

TABLE IV

(From Reference 9)

ADDED MASSES FOR THREE-DIMENSIONAL POTENTIAL FLOWS

(See Reference 9 or TABLE V for notation)

Sphere in translatory motion

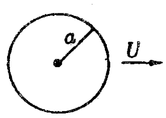

$$T = \frac{\pi}{3} \rho a^3 U^2, \qquad \text{as in Equation [127f]},$$

$$M' = \frac{4}{3} \pi \rho a^3, \qquad k = \frac{1}{2}.$$

Sphere moving perpendicularly to infinite rigid plane boundary, a/h small:

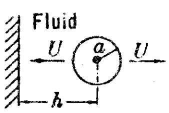

$$T = \frac{\pi}{3} \rho a^3 \left(1 + \frac{3}{8} \frac{a^3}{h^3} + \ldots\right) U^2, \qquad \text{as in Equation [130a]}$$

with $\alpha = 0$,

$$M' = \frac{4}{3} \pi \rho a^3, \qquad k = \frac{1}{2} \left(1 + \frac{3}{8} \frac{a^3}{h^3} + \ldots\right).$$

Only the force required to accelerate the sphere is considered here; see Section 130.

Sphere moving parallel to infinite rigid plane boundary, a/h small:

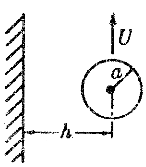

$$T = \frac{\pi}{3} \rho a^3 \left(1 + \frac{3}{16} \frac{a^3}{h^3} + \ldots\right) U^2, \qquad \text{as in Equation [130a]}$$

with $\alpha = 90$ deg,

$$M' = \frac{4}{3} \pi \rho a^3, \qquad k = \frac{1}{2} \left(1 + \frac{3}{16} \frac{a^3}{h^3} + \ldots\right).$$

Sphere moving past center of fixed spherical shell:

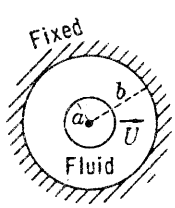

$$T = \frac{\pi}{3} \rho a^3 \frac{b^3 + 2a^3}{b^3 - a^3} U^2, \qquad \text{as in Equation [129e]},$$

$$M' = \frac{4}{3} \pi \rho a^3, \qquad k = \frac{1}{2} \frac{b^3 + 2a^3}{b^3 - a^3}.$$

TABLE IV (continued)

Prolate spheroid (or ovary ellipsoid), $a>b$; see Section 137:

Let e = eccentricity of sections through axis of symmetry,

$$\alpha_0 = \frac{1-e^2}{e^3}\left(\ln\frac{1+e}{1-e} - 2e\right),$$

$$\beta_0 = \frac{1-e^2}{e^3}\left(\frac{e}{1-e^2} - \frac{1}{2}\ln\frac{1+e}{1-e}\right).$$

(1) Translation "end on":

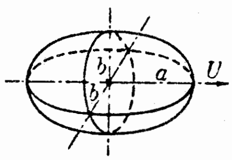

$$T = \frac{2}{3}\rho\pi\, ab^2 U^2 \frac{\alpha_0}{2-\alpha_0},$$

$$M = \frac{4}{3}\rho\pi\, ab^2, \qquad k = k_1 = \frac{\alpha_0}{2-\alpha_0}.$$

(2) Translation "broadside on":

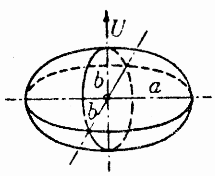

$$T = \frac{2}{3}\rho\pi\, ab^2 U^2 \frac{\beta_0}{2-\beta_0},$$

$$M = \frac{4}{3}\rho\pi\, ab^2, \qquad k = k_2 = \frac{\beta_0}{2-\beta_0}.$$

(3) Rotation about an axis perpendicular to axis of symmetry:

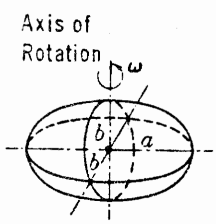

$$T = \frac{1}{2}k' I\omega^2, \qquad I = \frac{4}{15}\rho\pi\, ab^2(a^2+b^2),$$

$$k = k' = \frac{(a^2-b^2)^2(\beta_0-\alpha_0)}{(a^2+b^2)\,[2(a^2-\beta^2)-(a^2+b^2)(\beta_0-\alpha_0)]}.$$

See Table A

TABLE IV (continued)

TABLE A

Coefficients of Inertia for Prolate Sphéroid

a/b	k_1 Translation "end on"	k_2 Translation "broadside on"	k' Rotation about Minor Axis
1.00	0.500	0.500	0
1.50	0.305	0.621	0.094
2.00	0.209	0.702	0.240
2.51	0.156	0.763	0.367
2.99	0.122	0.803	0.465
3.99	0.082	0.860	0.608
4.99	0.059	0.895	0.701
6.01	0.045	0.918	0.764
6.97	0.036	0.933	0.805
8.01	0.029	0.945	0.840
9.02	0.024	0.954	0.865
9.97	0.021	0.960	0.883
∞	0	1.000	1.000

Oblate spheroid (or planetary ellipsoid), $a < b$, see Section 138, where $b = c$:

Let e = eccentricity of sections through axis of symmetry,

$$\alpha_0 = \frac{2}{e^3}(e - \sqrt{1-e^2}\ \sin^{-1}e),$$

$$\beta_0 = \frac{1}{e^3}[\ \sqrt{1-e^2}\ \sin^{-1}e\ - e\,(1-e^2)\,].$$

(1) Translation "broadside on" or parallel to axis:

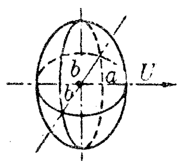

$$T = \frac{2}{3}\rho\pi\, ab^2 U^2\, \frac{\alpha_0}{2-\alpha_0},$$

$$M = \frac{4}{3}\rho\pi\, ab^2, \qquad k = k_1 = \frac{\alpha_0}{2-\alpha_0}.$$

CC BY

TABLE IV (continued)

(2) Translation "edge on" or perpendicular to axis:

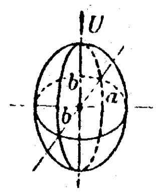

$$T = \frac{2}{3} \rho \pi a b^2 U^2 \frac{\beta_0}{2 - \beta_0},$$

$$M = \frac{4}{3} \rho \pi a b^2, \qquad k = k_2 = \frac{\beta_0}{2 - \beta_0}.$$

(3) Rotation about axis perpendicular to axis of symmetry:

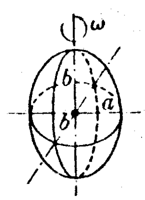

$$T = \frac{1}{2} k' I \omega^2, \qquad I = \frac{4}{15} \rho \pi a b^2 (a^2 + b^2),$$

$$k = k' = \frac{(b^2 - a^2)^2 (\alpha_0 - \beta_0)}{(a^2 + b^2) \left[2 (b^2 - a^2) - (a^2 + b^2)(\alpha_0 - \beta_0)\right]}.$$

See Table

TABLE 3

Coefficients of Inertia for Oblate Spheroid

b/a	k_2 Translation "edge on"	k_1 Translation "broadside on"	k' Rotation about Equatorial Axis
1.00	0.500	0.500	0
1.50	0.384	0.803	0.115
2.00	0.310	1.118	0.337
2.50	0.260	1.428	0.587
3.00	0.223	1.742	0.840
4.00	0.174	2.379	1.330
5.00	0.140	3.000	1.978
6.00	0.121	3.642	2.259
7.00	0.105	4.279	2.697
8.00	0 092	4.915	3.150
9.00	0.084	5.549	3.697
10.00	0.075	6.183	4.019
∞	0.000	∞	∞

TABLE IV (continued)

Circular disk in translation perpendicular to its faces:

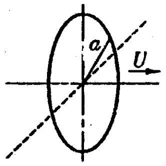

$$T = \frac{4}{3}\rho\, a^3 U^2,$$ as in Equation [138o′];

$$\frac{\text{(apparent increase in mass)}}{\text{(spherical mass of fluid of radius } a)} = \frac{2}{\pi}.$$

Circular disk rotating about a diameter; see Section 138:

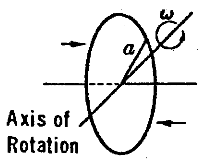

$$T = \frac{8}{45}\rho\, a^5 \omega^2,$$

$$\frac{\text{(apparent increase in moment of inertia)}}{\text{(moment of inertia of sphere of fluid of radius } a \text{ or } 8\rho\pi a^5/15)} = \frac{2}{3}.$$

Elliptic disk of ellipticity e in translation perpendicular to its faces, $a > b$; References (240) and (235):

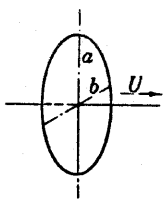

$$T = \frac{2\pi}{3E}\rho\, a^2 b\, U^2, \qquad e = \frac{1}{a}\sqrt{a^2 - b^2};$$

$$\frac{\text{(apparent increase in mass)}}{(\frac{4}{3}\rho\pi a^2 b = \text{ellipsoidal mass of fluid with axes } a, a, b)} = k'' = \frac{1}{E},$$

$$E = \int_0^{\pi/2} \sqrt{1 - e^2 \sin^2\theta}\; d\theta,$$ the complete elliptic integral of the second kind to modulus e; for table, see Peirce (20).

$a/b = 1$	1.25	1.5	1.75	2	2.5	3	4	6	9
$k'' = 0.637$	0.705	0.756	0.795	0.826	0.869	0.898	0.932	0.964	0.981

Ellipsoid, any ratio of the axes a, b, c; see Section 141:

Let $$\alpha_0 = abc\int_0^\infty \frac{d\lambda}{(a^2+\lambda)^{3/2}\,(b^2+\lambda)^{1/2}\,(c^2+\lambda)^{1/2}},$$

$$\beta_0 = abc\int_0^\infty \frac{d\lambda}{(a^2+\lambda)^{1/2}\,(b^2+\lambda)^{3/2}\,(c^2+\lambda)^{1/2}},$$

CC BY

TABLE IV (continued)

$$\gamma_0 = abc \int_0^\infty \frac{d\lambda}{(a^2+\lambda)^{1/2}\ (b^2+\lambda)^{1/2}\ (c^2+\lambda)^{3/2}} \,.$$

(1) Translation parallel to the a-axis:

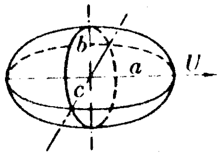

$$T = \frac{2}{3}\rho\pi\ abc\ \frac{\alpha_0}{2-\alpha_0} U^2,$$

$$M' = \frac{4}{3}\rho\pi\ abc, \qquad k = \frac{\alpha_0}{2-\alpha_0}$$

(2) Rotation about the a-axis:

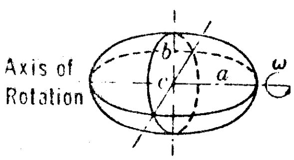

$$T = \frac{2}{15}\rho\pi\ abc\ \omega^2\ \frac{(b^2-c^2)^2\ (\gamma_0-\beta_0)}{2(b^2-c^2)+(b^2+c^2)\ (\beta_0-\gamma_0)}$$

$$I' = \frac{4}{15}\rho\pi\, abc(b^2+c^2), \qquad k' = \frac{(b^2-c^2)^2\ (\gamma_0-\beta_0)}{2(b^4-c^4)+(b^2+c^2)^2\ (\beta_0-\gamma_0)} \,.$$

For the expression of α_0, β_0, γ_0 in terms of elliptic integrals, see N.A.C.A. Report 210 by Tuckerman (235) or Volume I of Durand's Aerodynamic Theory (3). Some values of k and of k', distinguished by a subscript to denote the axis of the motion, were given by Zahm (174).

Fluid inside ellipsoidal shell rotating about its a-axis, any relative magnitudes of a, b, c (see last figure):

$$T = \frac{2}{15}\rho\pi\ abc\ \frac{(b^2-c^2)^2}{b^2+c^2}\ \omega^2 \qquad \text{as in Equation [140f],}$$

$$I' = \frac{4}{15}\rho\pi\ abc\ (b^2+c^2), \qquad k = \left(\frac{b^2-c^2}{b^2+c^2}\right)^2 .$$

TABLE IV (continued)

Solid of revolution formed by revolving about its axis of symmetry the limason defined by $r = b\,(s + \cos\theta)/(s^2 - 1)$ where b and s are constants. The curve for $s = 1$ is a cardioid. A few values of k are given by Bateman in Reference (240):

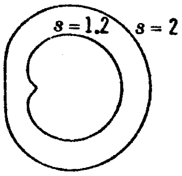

$s = 1$	1.1	1.2	2	3	∞
$k = 0.578$	0.573	0.569	0.548	0.527	0.500.

CC BY

TABLE V

(From Reference 9)

NOTATION FOR TABLES II AND IV : SEE ALSO REFERENCE 9

a, b, c	Radius of a circle or semiaxis of an ellipse or ellipsoid, or half-width or width of a lamina
e	Ellipticity
k	Coefficient of inertia, a dimensionless constant
In translation,	$k = \dfrac{\text{apparent increase in mass}}{\text{mass of displaced fluid}}$;
	$k = \dfrac{2T}{M'U^2}$ or $\dfrac{2T_1}{M_1'U^2}$.
In rotation,	$k = \dfrac{\text{apparent increase in moment of inertia}}{\text{moment of inertia of displaced fluid}}$;
	$k = \dfrac{2T}{I'\omega^2}$ or $\dfrac{2T_1}{I_1'\omega^2}$.
I'	Moment of inertia of displaced fluid rotating as a rigid body about the assumed axis of rotation
I_1'	See under T_1
M'	Mass of fluid displaced by body
M_1'	See under T_1
T	Kinetic energy of fluid
T_1, I_1', M_1':	Values of T, I', M' for fluid between two planes parallel to the motion and unit distance apart, in cases of two-dimentional motion
U	Velocity of translation of body
θ	An angle in radians
ρ	Density of the fluid, in dynamical units
ω	Angular velocity of rotation of a body, in radians per second.

The fluid is assumed to surround the body and to be of infinite extent and at rest at infinity, except where other conditions are indicated. In regard to units, see Sections 18, 147.